Published in final edited form as:
Int J Parasitol. 2009 April ; 39(5): 591–597. doi:10.1016/j.ijpara.2008.10.014.

Spatial heterogeneity of parasite co-infection:

Determinants and geostatistical prediction at regional scales

Simon Brooker[1,2,*] and **Archie C A Clements**[3]

[1]Department of Infectious and Tropical Diseases, London School of Hygiene and Tropical Medicine, Keppel Street, London WC1E 7HT, UK

[2]Malaria Public Health and Epidemiology Group, KEMRI-Wellcome Trust Collaborative Programme, Nairobi, Kenya

[3]School of Population Health, University of Queensland, Australia

Abstract

Multiple parasite infections are widespread in the developing world and understanding their geographical distribution is important for spatial targeting of differing intervention packages. We investigate the spatial epidemiology of mono-infection and co-infection with helminth parasites in East Africa and develop a geostatistical model to predict infection risk. The data used for the analysis was taken from standardised school surveys of *Schistosoma mansoni* and hookworm carried out between 1999 and 2005 in East Africa. Prevalence of mono-infection and co-infection was modelled using satellite-derived environmental and demographic variables as potential predictors. A Bayesian multinominal geostatistical model was developed for each infection category for producing maps of predicted co-infection risk. We show that heterogeneities in co-infection with *S. mansoni* and hookworm are influenced primarily by the distribution of *S. mansoni*, rather than the distribution of hookworm, and that temperature, elevation and distance to large water bodies are reliable predictors of the spatial large-scale distribution of co-infection. On the basis of these results, we developed a validated geostatistical model of the distribution of co-infection at a scale that is relevant for planning regional disease control efforts that simultaneously target multiple parasite species.

Keywords

parasite co-infection; helminths; hookworm; *Schistosoma mansoni*; Bayesian geostatistics; control programmes

Introduction

The heterogeneities involved in the transmission dynamics of parasitic diseases are well characterised and include aggregated distributions within host populations and marked spatial heterogeneity of infection (Anderson and May, 1985; Woolhouse et al., 1997; Smith et al., 2005). Such heterogeneities are influenced by multiple factors ranging from individual (genetic and/or behavioural) via household (demographic and socio-economic) to climatic and environmental influences. Recent studies, employing a combination of geographical information systems (GIS), remote sensing, geostatistics and mathematical modelling, have proven helpful in characterizing the spatial spread of infectious diseases (Russell et al.,

[*]**Corresponding author.** Department of Infectious and Tropical Diseases, London School of Hygiene and Tropical Medicine, Keppel Street, London WC1E 7HT. Email: simon.brooker@lshtm.ac.uk.

Europe PMC Funders Author Manuscripts

2005; Riley, 2007) and in determining linkages between spatial patterns and climatic and environmental factors (Raso et al., 2005; Clements et al., 2006a; Danson et al., 2006; Gemperli et al., 2006; Brooker, 2007; Diggle et al., 2007). This work has yielded new insights into the epidemiology and ecology of parasitic diseases at large geographical scales that had been difficult to address with traditional approaches. The work has also allowed disease distributions to be predicted robustly and helped inform where interventions should be geographically targeted on the basis of need and potential benefit (Brooker et al., 2006a; Clements et al., 2006b; Brooker, 2007).

However, infectious agents rarely occur in isolation, with co-infection with multiple species within host populations generally the norm (Petney and Andrews, 1998). Co-infection refers to when individuals harbour two infections simultaneously; this differs from mono-infection when individuals harbour only one infection, with regard to other infection species investigated (Raso et al., 2007). It is being increasingly recognized that co-infection has important ecological (Graham, 2008), epidemiological and clinical consequences (Cox, 2001; Mwangi et al., 2006; Pullan and Brooker, 2008). An ability to predict the large-scale geographical distribution of co-infection will have important implications for the design of disease control programmes. This is particularly true for integrated control programmes which simultaneously target multiple tropical diseases (Brooker and Utzinger, 2007; Hotez et al., 2007; WHO, 2007). Until recently, however, the spatial modelling of co-infection was largely ignored. Recent research has investigated the spatial distributions of co-infection with tuberculosis and HIV (Rodrigues et al., 2006) and *Schistosoma mansoni* and hookworm (Raso et al., 2006) as well as the co-endemicity of malaria and hookworm (Brooker et al., 2006b) and co-occurrence of diarrhoeal diseases and pneumonia (Fenn et al., 2005), and geostatistical models have been used to predict co-infection at local scales (Raso et al., 2006). To our knowledge, there have been no studies that have investigated the geography of co-infection at spatial scales relevant to planning large-scale control programmes, despite recent emphasis given to the distributional mapping of co-endemicity and co-infection (WHO, 2007).

In this paper we analyze empirical data from East Africa to investigate the heterogeneities and ecological correlates of mono- and co-infection with *S. mansoni* and hookworm among schoolchildren. We develop a Bayesian multinominal, geostatistical model of the geographical of co-infection, thereby helping inform planning of integrated disease control efforts in the region.

Data and methods

Data sources: outcome variable

Spatially referenced parasitological datasets were collated into a single database. Individual-level data were obtained in four separate school-based surveys conducted between 1999 and 2005 in a large, spatially contiguous area of East Africa, approximately 1260 km × 590 km, incorporating all of Uganda (Brooker et al., 2004; Kabatereine et al., 2004) and parts of northwest Tanzania (Clements et al., 2006b) and southwest Kenya (Brooker et al., 2001; Koukounari et al., 2008). No previous mass treatment with anthelmintic drugs had been undertaken in any of the schools, and although seasonal dynamics in transmission stages may occur, such fluctuations may be of little significance to the overall parasite equilibrium within communities. This is because the life-span of adult worms is typically much longer (1-10 years) than the periods in the year during which the basic reproductive number (R_o) is less than unity, and R_o will on average be greater than one, maintaining overall endemicity. For this reason, spatial variability in long-term synoptic environmental factors will have a greater influence on transmission success and patterns of helminth infection than seasonal variability in a location.

Detailed descriptions of survey design and study methods are provided in the original references. In brief, stool samples were collected from each schoolchild and processed using standard parasitological methods. Presence of infection was based on the microscopic examination of two Kato-Katz thick smears made from a single stool specimen - a child was considered positive for *S. mansoni* or hookworm if at least one egg was detected on examination of either smear. The outcome variable was infection status grouped into four categories: (i) no infection; (ii) *S. mansoni* mono-infection; (iii) hookworm mono-infection; and (iv) co-infection with *S. mansoni* and hookworm.

Data sources: demography and environmental variables

Information on age and sex was collected by interview and confirmed against school registers. Age was categorised into approximately equally sized groups: ≤8, 9-10, 11-13 and ≥14 years. The geographical position of schools was determined using different global positioning systems. A range of environmental data were collated including: satellite-derived mean land surface temperature (LST) and normalized difference vegetation index (NDVI) for 1982-2000, obtained from the National Oceanographic and Atmospheric Administration's Advanced Very High Resolution Radiometer; elevation, obtained from an interpolated digital elevation model from the Global Land Information System (GLIS) of the United States Geological Survey (Hay et al., 2006); distance to perennial inland water-bodies; and degree of urbanisation (urban, peri-urban, rural and extreme rural) (Hay et al., 2005), with urban and peri-urban classes grouped into a single class due to the small size of urban areas relative to the study area. The values for each of the environmental variables at the location of each of the schools surveyed were calculated in the GIS ArcView version 9 (ESRI, Redlands, CA., USA)

Ethical approval

Ethical approval was obtained from the following ethic review boards: National Institute of Medical Research, Tanzania; National Health Service Local Research Ethics Committee of St Mary's Hospital, London; Ministry of Health, Uganda; Kenyatta National Hospital, Kenya; London School of Hygiene and Tropical Medicine. In the Kenya studies, meetings were held in participating schools prior to the surveys to explain the nature and purpose of the study to parents or legal guardians, and written informed consent was obtained. In the Tanzania and Uganda studies, passive consent was sought, thereby parents were informed of the study prior to the school visit through parent-teacher association meetings, when they had the opportunity to ask questions about the study, be told that participation is voluntary and that they can withdraw their child from the study at any time. In all of the studies, verbal assent to participate in the survey was also sought from the child at the time of sampling. Following the surveys, all children received treatment with albendazole (400mg). Treatment with praziquantel (40 mg/kg) was provided only children found to be infected with schistosomiasis or enrolled in schools where the overall prevalence was >=50%.

Statistical analysis

Heterogeneity was initially assessed on the basis of the frequency distributions of parasite prevalence. Maps of prevalence were created in GIS ArcView version 9 (ESRI, Redlands, CA., USA). Subsequently, univariate multinomial regression models were developed in Stata version 10 (Stata, College Station, TX., USA) to investigate the relationship between the outcome variable and covariates. Covariates significant at a 0.2 significance level were included into a Bayesian spatial multinomial logistic regression model. This model was based on the principle of model-based geostatistics (Diggle et al., 1998), where the model has two components: a deterministic component consisting of school-level climatic and individual-level fixed effects; and a stochastic component based on a stationary

geostatistical model of the spatial covariance structure. Separate regression coefficients and spatial autocorrelation parameters were estimated for each of the outcome categories.

The model was developed in WinBUGS version 14 (MRC Biostatistics Unit, Cambridge, UK). The individual data were aggregated into age and gender groups and by location. Using four infection outcome groups (1 = no infection, 2 = *S. mansoni* mono-infection, 3 = hookworm mono-infection and 4 = *S.mansoni*-hookworm co-infection), we assumed

$$Y_{ijk} \sim \text{Multinomial}\left(p_{ijk}, n_{ijk}\right),$$

$$p_{ijk} = \frac{\phi_{ijk}}{\sum_{k} n_{ijk}},$$

where Y_{ijk} is the observed number positive, n_{ijk} is the number tested and p_{ijk} is probability of infection at location *i,* in age-gender group *j*, infection outcome group *k*, where φ_{ij1} was constrained to equal one, and for the other outcome groups:

$$log\left(\phi_{ijk}\right) = \alpha_k + \sum_{N=1,k}^{T} \beta_{Nk} \times x_{Nijk} + \theta_{ik},$$

where α_k is the outcome group-specific intercept, $\sum_{N=1,k}^{T} \beta_{Nk} \times x_{Nijk}$ is a vector of T covariates with outcome group-specific coefficients and θ_{ik} are outcome group-specific geostatistical random-effects defined by an isotropic powered exponential spatial correlation function:

$$f\left(d_{ij};\phi\right) = \exp\lfloor -\left(\phi d_{ij}\right)\rfloor,$$

where d_{ij} are the distances between pairs of points *i* and *j*, and φ is the rate of decline of spatial correlation per unit of distance. Non-informative priors were specified for the intercepts (uniform prior with bounds - ∞ and ∞) and the coefficients (normal prior with mean = 0 and precision = 1×10^{-4}). The prior distribution of φ was also uniform with upper and lower bounds set at 0.06 and 50. The θ_{ik} were given a non-informative prior gamma distribution.

Three chains of the models were run consecutively. A burn-in of 1,000 iterations was allowed, followed by 10,000 iterations where values for the intercept and coefficients were stored. Diagnostic tests for convergence of the stored variables were undertaken, including visual examination of history and density plots of the three chains. Convergence was successfully achieved after 10,000 iterations and the posterior distributions of model parameters were combined across the three chains and summarized using descriptive statistics.

Samples from the posterior distributions of the coefficients from the model were used to produce prediction maps of co-infection on a 0.2×0.2 decimal degree (approximately 24.4×24.4 km) grid covering the study area, using Bayesian kriging. Prediction at non-sampled locations was done in WinBUGS using the *spatial.unipred* command.

Model validation

Validation of predicted school-level prevalence of co-infection was undertaken by partitioning the data into four random sets and running the model using three of the four sets and validating the model with the remaining set. Four separate models were run using different combinations of three training sets and one validation set. The accuracy of the prediction was determined in terms of sensitivity and specificity and by the area under curve (AUC) of a receiver-operating characteristic (ROC) curve to determine the ability of the model predictions to discriminate between a true prevalence of 0% versus >0%, <10% versus >=10%, and <20% versus >=20%. As a general rule, an AUC between 0.5-0.7 indicates a poor discriminative capacity; 0.7-0.9 indicate a reasonable capacity; and >0.9 indicate a very good capacity. Four different estimates of AUC were derived, and an average AUC was presented.

Results

Data on both *S. mansoni* and hookworm were available for 27,729 schoolchildren from 395 schools. Overall, 7.9% of children were infected with only *S. mansoni* infection; 40.5% of children had only hookworm infection; and 8.1% of children harbored both infections concurrently. Infection patterns were broadly similar between the sexes but males were more co-infected compared to females (11.6% vs 9.4%, Pearson $Chi^2 = 35.7$, $p<0.001$). Patterns of co-infection differed markedly between study areas (Table 1) and between schools (Figure 1a). The frequency distribution of *S. mansoni* mono-infection was highly skewed, with 80% of schools having a prevalence <10%. By contrast, the distribution of hookworm mono-infection was generally symmetrical, with most schools having prevalences between 40 and 69.9 %. Following the pattern of *S. mansoni* mono-infection, the frequency distribution of co-infection was also highly skewed. Figure 1b presents the geographical distribution of mono- and co-infection by school and shows that co-infection prevalence was highest along the shores of Lake Victoria and Lake Albert.

Table 2 presents the results of the geostatistical Bayesian multinomial logistic regression model. The rate of decline in spatial correlation (φ) and the variance of the geostatistical random effect were more similar for *S. mansoni* mono-infection and co-infection than for hookworm mono-infection and co-infection. The slightly lower φ for *S. mansoni* mono-infection and co-infection indicated that spatial correlation occurred over longer distances than hookworm mono-infection prevalence (i.e. spatial clusters were slightly larger). Additionally, the much higher variance of the geostatistical random effect for *S. mansoni* mono-infection and co-infection indicated a higher tendency towards spatial clustering than for hookworm. In other words, there was stronger evidence for spatial variability of *S. mansoni* mono-infection and co-infection than for hookworm mono-infection.

Individual-level and environmental variables were significantly associated with the risk of each type of infection. Risk increased with age and was lower for females. Negative associations were observed between *S. mansoni* mono-infection and elevation, distance to permanent water body, and rural areas (category 3). Risk of hookworm mono-infection was negatively associated with LST and elevation. Finally, all of the included covariates were associated with co-infection, except rural (category 3). By using a true co-infection prevalence threshold of >0% (i.e. the ability to predict the occurrence of co-infection), the average AUC of the four validation runs was 0.88. Using a true prevalence threshold of >10%, the average AUC was 0.92, and for a prevalence threshold of >20%, the AUC was 0.93.

On the basis of these models and validation, it was possible to predict the distributions of mono- and co-infection (Figure 2). The prevalence of *S. mansoni* mono-infection was

greatest along the shores of Lake Victoria, Lake Albert and the Albert Nile (Figure 2a). The predicted prevalence of hookworm mono-infection was more homogeneously distributed, with low prevalence predicted in northeast Uganda and parts of Tanzania (Figure 2b). The predicted distribution of *S. mansoni*-hookworm co-infection was broadly similar to *S. mansoni* mono-infection in northwest and southeast Uganda (Figure 2c); however, there were areas of high predicted co-infection prevalence in central Uganda and the southwestern shores of Lake Victoria. Figure 2d presents the standard deviation of the co-infection prediction and shows that the standard deviation was greatest in areas of high prevalence of co-infection and in areas away from sampled locations.

Figure 3 shows the spatial random effect for co-infection which represents the variation in co-infection that was not explained by the model covariates yet is spatially-structured. Areas of high residual co-infection occurred in northern Uganda, western Kenya and the southwest shores of Lake Victoria.

Discussion

Biological phenomena rarely occur in isolation, and this is certainly true for parasite species within and between host populations. An ability to predict spatial distributions of co-infection will enhance our epidemiological understanding of the co-endemicity of parasite species and can provide an evidence-base for the spatial targeting of large-scale integrated control programmes (Brooker and Utzinger, 2007; WHO, 2007). Here we show it is possible to predict the regional distribution of mono- and co-infection with *S. mansoni* and with hookworm, two of the most common and geographically widespread tropical parasitic diseases, in East Africa.

Most existing studies of the spatial epidemiology of parasitic diseases focus on single species and highlight the marked spatial heterogeneity in patterns of infection (Raso et al., 2005; Brooker, 2007; Clennon et al., 2007; Sogoba et al., 2007). We demonstrate that the distribution of both *S. mansoni* mono-infection and co-infection is extremely focal, exhibiting a highly skewed frequency distribution and a marked spatial dependency. In contrast, the distribution of hookworm mono-infection was more symmetrical and geographically homogeneous. The generally similar patterns of *S. mansoni* mono-infection and co-infection suggest that the spatial distribution of co-infection is driven primarily by the distribution of *S. mansoni*, rather than the distribution of hookworm. The transmission of *S.mansoni* depends on the distribution and density of its intermediate hosts, freshwater snails. The population dynamics of snails are affected by a range of climatic and environmental factors, primarily temperature, elevation and distance to large water bodies (Sturrock, 1993; Brooker and Michael, 2000; Yang et al., 2005). These variables are readily incorporated within a GIS and have previously been used to predict spatial distributions of schistosomiasis (reviewed in Brooker, 2007). Our modelling shows that it is also possible to predict spatial patterns of co-infection on the basis of key climatic and environmental variables (Figure 2c).

There were some interesting exceptions to the role of *S. mansoni* in co-infection dynamics, especially in central Uganda where the high co-infection prevalence arises from the high prevalence of hookworm. This may reflect the differential environmental determinants of each parasite species in different parts of the study area. It is also worth emphasizing that the areas of high residual co-infection (Figure 3) highlight potentially important, unmeasured covariates, which may influence transmission patterns. These might include socio-economic status, which has shown previously to be associated with *S. mansoni*-hookworm co-infection at small geographical scales (Raso et al., 2006). However, high-resolution poverty maps at regional scales are lacking since poverty data are available only at geographically

aggregated levels and are often country-specific (Benson et al., 2005; Kristjanson et al., 2005; Noor et al., 2006). Another possible determinant of polyparasitism, which is also poorly mapped, is access to clean water and sanitation (Singer and Caldas de Castro, 2007); however, water and sanitation mapping is only starting to develop.

Our adopted approach has a number of advantages and limitations. The Bayesian framework allows for the explicit inclusion of spatial structure and reliable uncertainty estimation (Diggle et al., 1998; Clyde and George, 2004). The use of a single Kato-Katz smear to detect infection is a limitation since this approach is known to lack sensitivity and specificity, especially in the detection of light *S. manosni* infections (de Vlas and Gryseels, 1992), and multiple smears are recommended where possible (Booth et al., 2003). However, many of the surveys included in the present analysis were conducted in isolated communities over large geographical distances, employing mobile survey teams, thereby preventing the collection of multiple samples. Delays in processing samples after collection may also introduce bias, although this is more important for hookworm than for *S. mansoni* (Dacombe et al., 2007). Nonetheless, the fact that the same diagnostic approach was used in the included surveys at least makes the data comparable, if subject to the same biases.

The derived maps can help inform policy and decision making concerning large-scale parasite control strategies. Current efforts to control schistosomiasis and hookworm typically focus on the school-age population since much of the morbidity caused by helminth infections occur in this sub-population and school-based treatment delivery programmes offer major cost advantages (Bundy et al., 2006). These programmes deliver mass co-administration of praziquantel to treat schistosomiasis and benzimidazole anthelmintics (albdendazole or mebendazole), to treat hookworm and other soil-transmitted helminth infections, in areas where both types of infections are prevalent (Bundy et al., 1991). There is a need, therefore, to identify the most appropriate mix of interventions in different areas according to patterns of mono- and co-infection (Bundy et al., 1991; Raso et al., 2007); blanket treatment of praziquantel and benzimidazoles may lead to treating large numbers of individuals unnecessarily. Our models were aimed at national policy and decision making, and argue for a spatially targeted approach to control of schistosomiasis and co-infection, but widespread, mass control of hookworm within the broad limits of its geographical range.

This study provides a reasonable prediction of mono- and co-infection with two of the widespread and important helminth infections that infect humans in the developing world. Our adopted approach may well apply to other combinations of co-infection where a geographically targeted approach to control is required. For example, there has been increased advocacy for the logistic and economic benefits of integrating national control programmes targeting a range of so-called neglected tropical diseases, including schistosomiasis, soil-transmitted helminths, lymphatic filariasis and onchocerciasis (Richard et al,. 2006; Hotez et al., 2007). There are also calls to investigate the potential of a combined approach to helminth-malaria control (Brooker et al., 2007). It will therefore become increasingly important to understand the main drivers of co-infection with different species. For example, although malaria and hookworm occur coincidentally over much of sub-Saharan Africa (Brooker et al., 2006b), it remains unclear whether the climatic and environmental drivers of each disease are the same, similar or spatially co-incident. In turn, there is a requirement for better empirical data on patterns of co-infection and to develop more models of co-infection for a range of tropical diseases in varying transmission settings. There is also a need for spatially explicit economic models to be developed, which include estimates of programme cost and cost-effectiveness in order to support decision making.

Acknowledgments

We thank the schoolchildren and their teachers who participated in the surveys. We also thank Giovanna Raso and Adrian Barnett, University of Queensland, for providing statistical advice on the spatial models, Nicholas Lwambo (Tanzania), Narcis Kabatereine (Uganda), Benson Estambale, Sian Clarke, Ted Miguel and Kiambo Njagi (Kenya) for leading the survey teams that collected the parasitological data, Andrew Tatem for providing much of the climate and demographic data used in the models, and Don Bundy and Simon Hay for providing comments on an earlier draft. This work was supported by the Wellcome Trust through a Career Development Fellowship (081673) to Simon Brooker.

References

Anderson RM, May RM. Helminth infections of humans: mathematical models, population dynamics, and control. Adv Parasitol. 1985; 24:1–101. [PubMed: 3904343]

Benson T, Chamberlin J, Rhinehart I. An investigation of the spatial determinants of the local prevalence of poverty in rural Malawi. Food Policy. 2005; 30:532–550.

Booth M, Vounatsou P, N'goran EK, Tanner M, Utzinger J. The influence of sampling effort and the performance of the Kato-Katz technique in diagnosing *Schistosoma mansoni* and hookworm co-infections in rural Côte d'Ivoire. Parasitology. 2003; 127:525–531. [PubMed: 14700188]

Brooker S, Michael E. The potential of geographical information systems and remote sensing in the epidemiology and control of human helminth infections. Adv Parasitol. 2000; 47:245–288. [PubMed: 10997209]

Brooker S, Miguel EA, Moulin S, Waswa P, Namunyu R, Guyatt H, Bundy DAP. The potential of rapid screening methods for *Schistosoma mansoni* in Western Kenya. Ann Trop Med Parasitol. 2001; 95:343–351. [PubMed: 11454244]

Brooker S, Kabatereine NB, Tukahebwa EM, Kazibwe F. Spatial analysis of the distribution of intestinal nematode infections in Uganda. Epi Infect. 2004; 132:1065–1071.

Brooker S, Clements ACA, Bundy DAP. Global epidemiology, ecology and control of soil-transmitted helminth infections. Adv Parasitol. 2006a; 62:223–265.

Brooker S, Clements ACA, Hotez PJ, Hay SI, Tatem AJ, Bundy DAP, Snow RW. The co-distribution of *Plasmodium falciparum* and hookworm in African schoolchildren. Malaria J. 2006b; 5:99.

Brooker S. Spatial epidemiology of human schistosomiasis in Africa: risk models, transmission dynamics and control. Trans R Soc Trop Med Hyg. 2007; 101:1–8. [PubMed: 17055547]

Brooker S, Akhwale W, Pullan R, Estambale B, Clarke SE, Snow RW, Hotez PJ. Epidemiology of Plasmodium-helminth co-infections in Africa: population at risk, potential impact on anemia and prospects for combined control. Am J Hyg Trop Med. 2007; 77:S88–S98.

Brooker S, Utzinger J. Integrated disease mapping in a polyparasitic world. Geospat Health. 2007; 1:141–6. [PubMed: 18686239]

Bundy DAP, Chandiwana SK, Homeida MMA, Yoon S, Mott KE. The epidemiological implications of a multiple-infection approach to the control of human helminth infections. Trans R Soc Trop Med Hyg. 1991; 85:274–276. [PubMed: 1887492]

Bundy, DAP.; Shaeffer, S.; Jukes, M.; Beegle, K.; Gillespie, A.; Drake, L.; Seung-hee Frances, Lee; Hoffman, AM.; Jones, J.; Mitchell, A.; Wright, C.; Barcelona, D.; Camara, B.; Golmar, C.; Savioli, L.; Takeuchi, T.; Sembene, M. Disease Control Priorities in Developing Countries. Jamison, D.; Breman, JG.; Measham, AR.; Alleyne, G.; Claeson, M.; Evans, DB.; Jha, P.; Mills, A.; Musgrove, P., editors. The World Bank and Oxford University; New York: 2006. p. 1091-1108.

Clements ACA, Moyeed R, Brooker S. Bayesian geostatistical prediction of the intensity of infection with *Schistosoma mansoni* in East Africa. Parasitology. 2006a; 133:711–719. [PubMed: 16953953]

Clements ACA, Lwambo NJS, Blair L, Nyandindi U, Kaatano G, Kinung'hi S, Webster JP, Fenwick A, Brooker S. Bayesian spatial analysis and disease mapping: tools to enhance planning and implementation of a schistosomiasis control programme in Tanzania. Trop Med Int Hlth. 2006b; 11:490–503.

Clennon JA, Mungai PL, Muchiri EM, King CH, Kitron U. Spatial and temporal variations in local transmission of *Schistosoma haematobium* in Msambweni, Kenya. Am J Trop Med Hyg. 2006; 75:1034–1041. [PubMed: 17172362]

Clyde M, George EI. Model uncertainty. Statist Sci. 2004; 19:81–94.

Cox FE. Concomitant infections, parasites and immune responses. Parasitology. 2001; 122(Suppl):S23–S38. [PubMed: 11442193]

Dacombe RJ, Crampin AC, Floyd S, Randall A, Ndhlovu R, Bickle Q, Fine PE. Time delays between patient and laboratory selectively affect accuracy of helminth diagnosis. Trans R Soc Trop Med Hyg. 2007; 101:140–5. [PubMed: 16824566]

Danson FM, Giraudoux P, Craig PS. Spatial modelling and ecology of Echinococcus multilocularis transmission in China. Parasitol Int. 2006; 55(Suppl):S227–S231. [PubMed: 16371253]

Diggle P, Tawn JA, Moyeed R. Model-based geostatistics. App Stat. 1998; 47:299–350.

Diggle PJ, Thomson MC, Christensen OF, Rowlingson B, Obsomer V, Gardon J, Wanji S, Takougang I, Enyong P, Kamgno J, Remme JH, Boussinesq M, Molyneux DH. Spatial modelling and the prediction of *Loa loa* risk: decision making under uncertainty. Ann Trop Med Parasitol. 2007; 101:499–509. [PubMed: 17716433]

Fenn B, Morris SS, Black RE. Comorbidity in childhood in northern Ghana: magnitude, associated factors, and impact on mortality. Int J Epidemiol. 2005; 34:368–375. [PubMed: 15764695]

Gemperli A, Vounatsou P, Sogoba N, Smith T. Malaria mapping using transmission models: application to survey data from Mali. Am J Epidemiol. 2006; 163:289–297. [PubMed: 16357113]

Graham AL. Ecological rules governing helminth-microparasite coinfection. Proc Natl Acad Sci USA. 2008; 105:566–570. [PubMed: 18182496]

Hay SI, Guerra CA, Tatem AJ, Atkinson PM, Snow RW. Urbanization, malaria transmission and disease burden in Africa. Nature Rev Microbiology. 2005; 3:81–90.

Hay SI, Tatem AJ, Graham AJ, Goetz SJ, Rogers DJ. Global environmental data for mapping infectious disease distribution. Adv Parasitol. 2006; 62:37–77. [PubMed: 16647967]

Hotez PJ, Molyneux DH, Fenwick A, Kumaresan J, Sachs SE, Sachs JD, Savioli L. Control of neglected tropical diseases. N Engl J Med. 2007; 357:1018–27. [PubMed: 17804846]

Kabatereine NB, Brooker S, Tukahebwa EM, Kazibwe F, Onapa A. Epidemiology and geography of *Schistosoma mansoni* in Uganda: implications for planning control. Trop Med Int Hlth. 2004; 9:372–380.

Koukounari A, Estambale BBA, Njagi JK, Cundill B, Jukes MJ, Otido J, Clarke SE, Brooker S. Relationships between anaemia and parasitic infections in African schoolchildren: a Bayesian hierarchical modelling approach. Int J Parasitol. in press.

Kristjanson P, Radeny M, Baltenweck I, Ogutu J, Notenbaert A. Livelihood mapping and poverty correlates at a meso-level in Kenya. Food Policy. 2005; 30:568–583.

Mwangi TW, Bethony J, Brooker S. Worms and malaria interactions: an epidemiological viewpoint. Ann Trop Med Parasitol. 2006; 100:551–570. [PubMed: 16989681]

Noor AM, Omumbo JA, Amin AA, Zurovac D, Snow RW. Wealth, mother's education and physical access as determinants of retail sector net use in rural Kenya. Malaria J. 2006; 5:5.

Petney TN, Andrews RH. Multiparasite communities in animals and humans: frequency, structure and pathogenic significance. Int J Parsitol. 1998; 28:377–393.

Pullan R, Brooker S. The health impact of polyparasitism in humans: are we under-estimating the burden of parasitic diseases? Parasitology. 2008; 135:783–794. [PubMed: 18371242]

Raso G, Matthys B, N'Goran EK, Tanner M, Vounatsou P, Utzinger J. Spatial risk prediction and mapping of *Schistosoma mansoni* infections among schoolchildren living in western Côte d'Ivoire. Parasitology. 2005; 131:97–108. [PubMed: 16038401]

Raso G, Vounatsou P, Singer BH, N'Goran EK, Tanner M, Utzinger J. An integrated approach for risk profiling and spatial prediction of *Schistosoma mansoni*-hookworm coinfection. Proc Natl Acad Sci USA. 2006; 103:6934–6939. [PubMed: 16632601]

Raso G, Vounatsou P, McManus DP, Utzinger J. Bayesian risk maps for *Schistosoma mansoni* and hookworm mono-infections in a setting where both parasites co-exist. Geospatial Health. 2007; 2:85–96. [PubMed: 18686258]

Richards FO Jr, Eigege A, Miri ES, Jinadu MY, Hopkins DR. Integration of mass drug administration programmes in Nigeria: The challenge of schistosomiasis. Bull World Health Organ. 2006; 84:673–6. [PubMed: 16917658]

Riley S. Large-scale spatial-transmission models of infectious disease. Science. 2007; 316:1298–1301. [PubMed: 17540894]

Rodrigues AL, Ruffiono-Netto A, de Castilho EA. Spatial distribution of *M. Tuberculosis*/HIV coinfection in São Paulo State, Brazil, 1991-2001. Rev Saúde Pública. 2006; 40:1–6.

Russell CA, Smith DL, Childs JE, Real LA. Predictive spatial dynamics and strategic planning for raccoon rabies emergence in Ohio. PLoS Biol. 2005; 3:e88. [PubMed: 15737065]

Singer BH, Caldas de Castro M. Bridges to sustainable tropical health. Proc Natl Acad Sci USA. 2007; 104:16038–16043. [PubMed: 17913894]

Smith DL, Dushoff J, Snow RW, Hay SI. The entomological inoculation rate and *Plasmodium falciparum* infection in African children. Nature. 2005; 438:492–495. [PubMed: 16306991]

Sogoba N, Vounatsou P, Doumbia S, Bagayoko M, Touré MB, Sissoko IM, Traore SF, Touré YT, Smith T. Spatial analysis of malaria transmission parameters in the rice cultivation area of Office du Niger, Mali. Am J Trop Med Hyg. 2007; 76:1009–1015. [PubMed: 17556602]

Sturrock, RF. Human Schistosomiasis. Jordan, P.; Webbe, G.; Sturrock, RF., editors. CAB International; Wallingford: 1993. p. 33-85.

Woolhouse ME, Dye C, Etard JF, Smith T, Charlwood JD, Garnett GP, Hagan P, Hii JL, Ndhlovu PD, Quinnell RJ, Watts CH, Chandiwana SK, Anderson RM. Heterogeneities in the transmission of infectious agents: implications for the design of control programmes. Proc Natl Acad Sci USA. 1997; 7:338–342. [PubMed: 8990210]

de Vlas SJ, Gryseels B. Underestimation of *Schistosoma mansoni* prevalences. Parasitol Today. 1992; 8:274–7. [PubMed: 15463638]

WHO. Report of the first meeting of WHO Strategic and Technical Advisory Group on Neglected Tropical Diseases. World Health Organization; Geneva: 2007. WHO/CDS/NTD/2007.2

Yang GJ, Vounatsou P, Zhou XN, Utzinger J, Tanner M. A review of geographic information system and remote sensing with applications to the epidemiology and control of schistosomiasis in China. Acta Tropica. 2005; 96:117–29. [PubMed: 16112638]

Europe PMC Funders Author Manuscripts

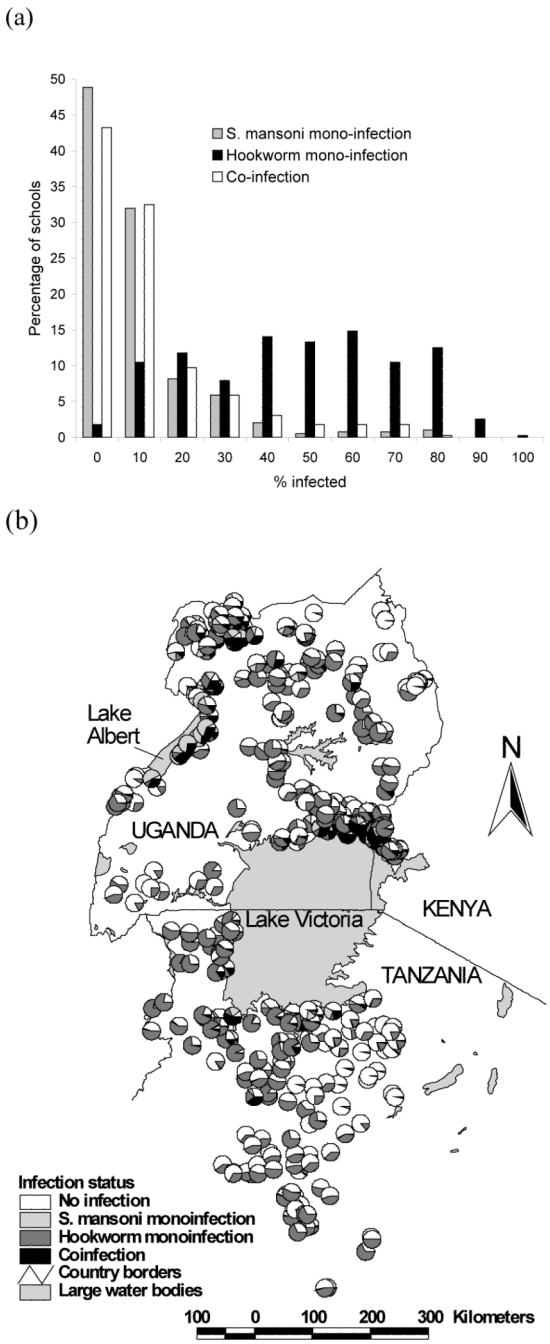

Figure 1.
(a) Frequency distribution and (b) geographical distribution of mono- and co-infection with *Schistosoma mansoni* and hookworm among 27,729 schoolchildren from 395 schools in East Africa.

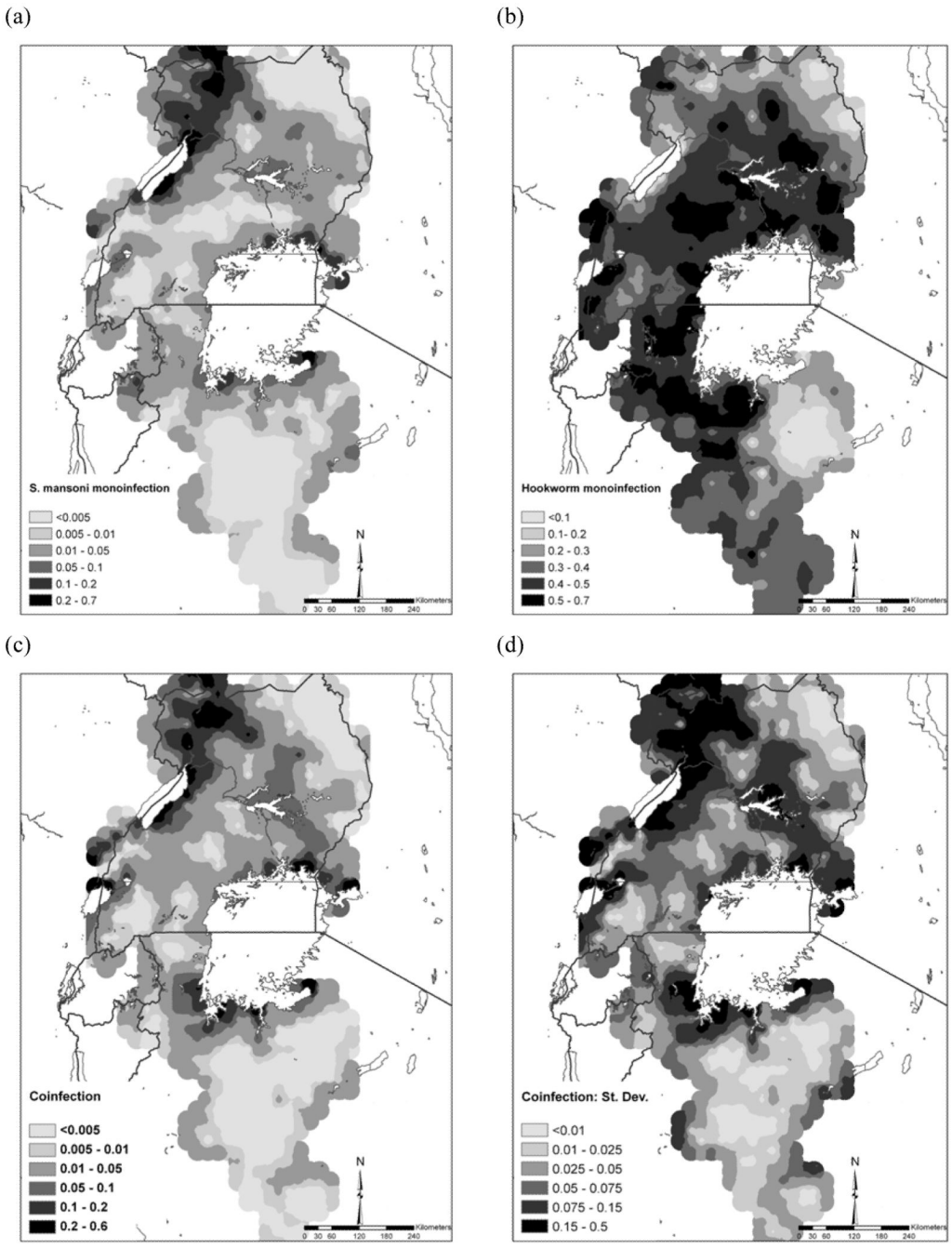

Figure 2.

Predicted distribution of (a) *S. mansoni* mono-infection, (b) hookworm mono-infection, (c) *S.mansoni*-hookworm co-infection, and (d) standard deviation of the predicted *S.mansoni*-hookworm co-infection among schoolchildren in East Africa. Note the different legend categories for each map for presentation purposes.

Europe PMC Funders Author Manuscripts

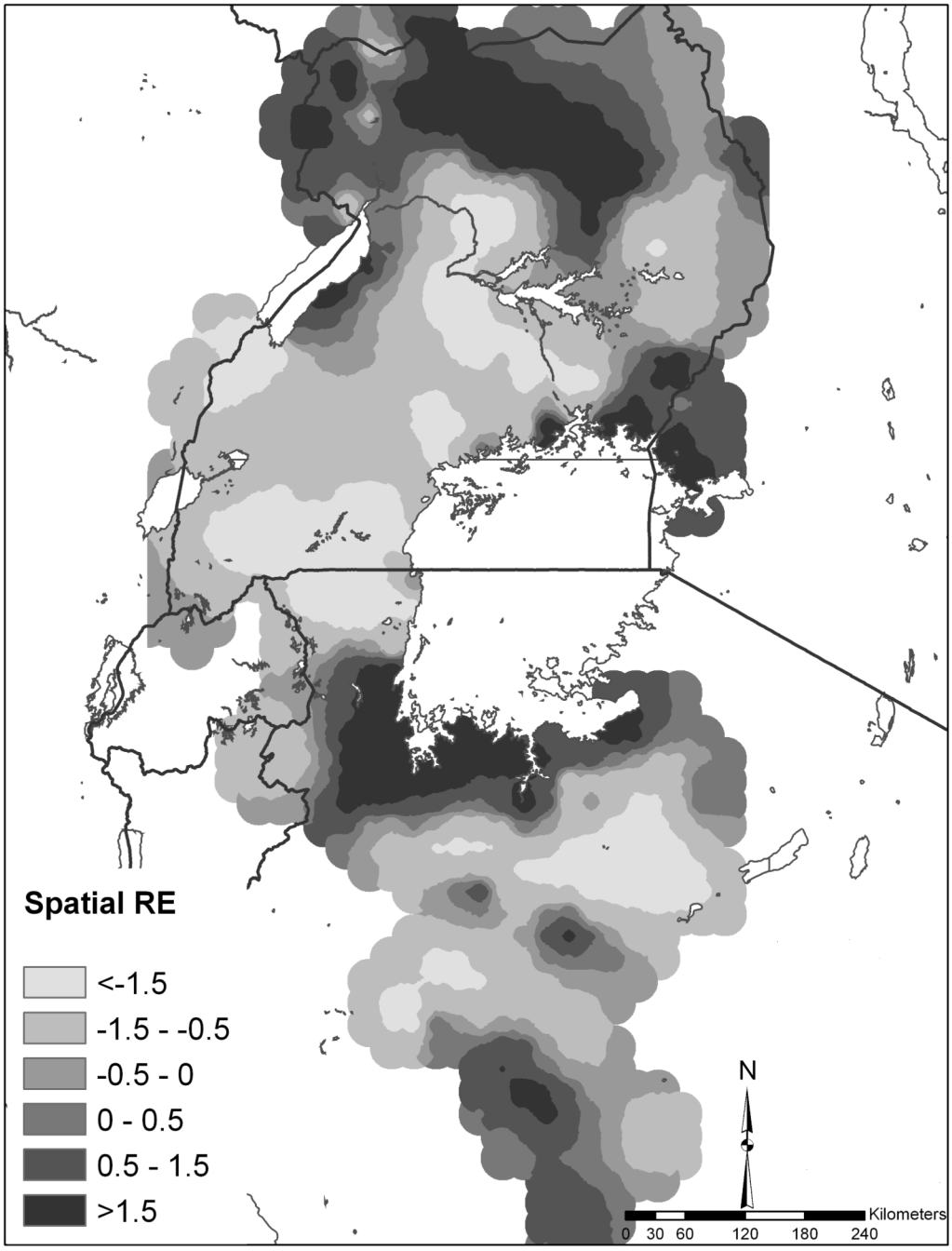

Figure 3.

Europe PMC Funders Author Manuscripts

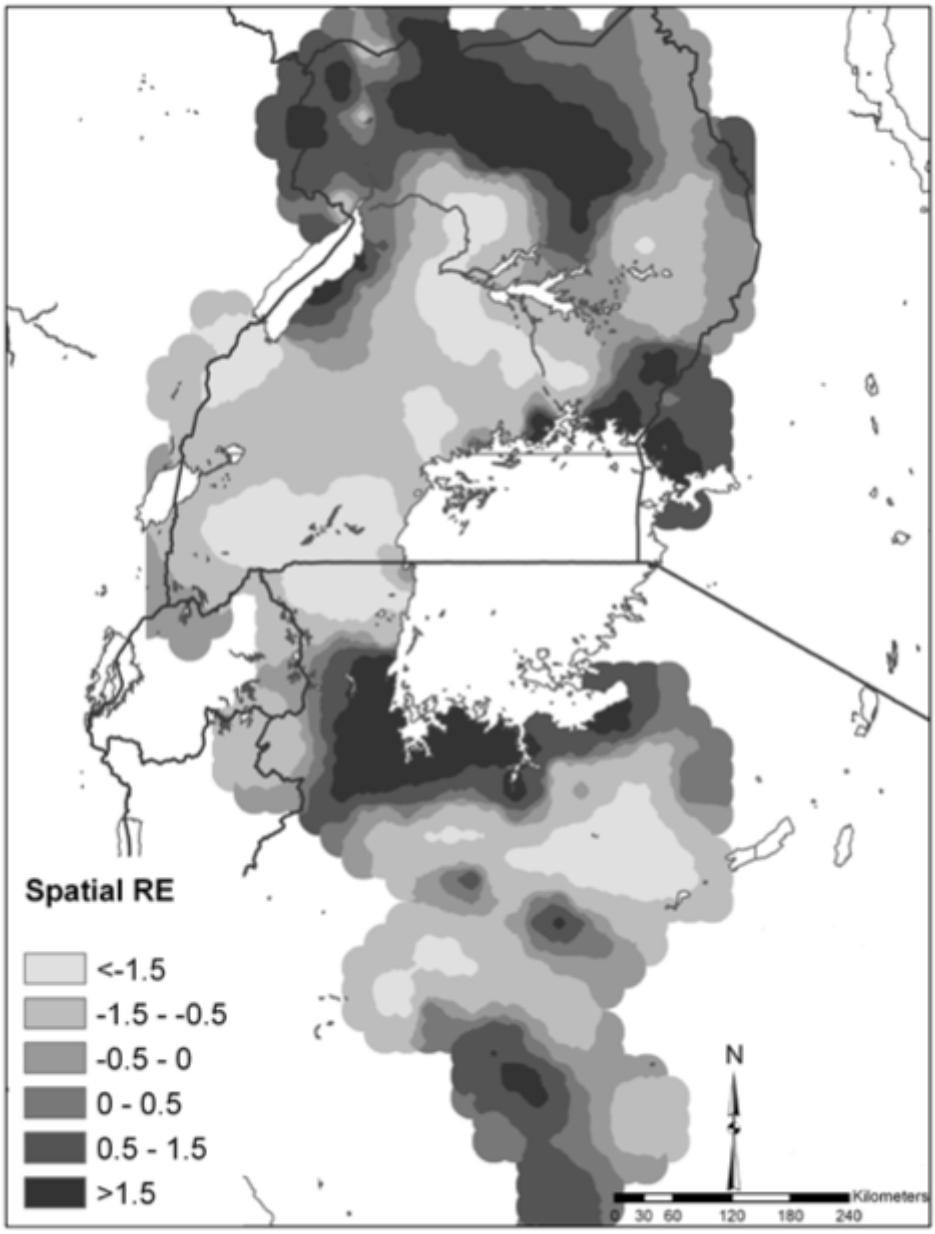

Figure 4.
Map of the spatial random-effect (RE) component of the predictions for *S. mansoni*-hookworm co-infection.

Europe PMC Funders Author Manuscripts

Table 1

Prevalence (% infected) of infection and mono- and co-infection with *Schistosoma mansoni* and hookworm among 27,729 schoolchildren from 395 schools in East Africa

	Study region				Total (range by school)
	Bondo, Kenya 2005	**Busia, Kenya 2000**	**NW Tanzania 2005**	**Uganda 1999-2002**	
No. of children	1,092	1,677	8,617	16,343	27,729
S. mansoni	14.3	22.3	4.4	26.1	18.7 (0-97.3)
Hookworm	47.2	77.1	48.0	50.2	51.0 (0-95.7)
No infection	44.9	16.5	50.3	38.0	40.9 (0-100)
S. mansoni mono-infection	7.9	6.4	1.7	11.8	8.1 (0-80.0)
Hookworm mono-infection	40.8	61.2	45.2	35.9	40.5 (0-91.6)
Co-infection	6.4	15.9	2.8	14.3	10.5 (0-71.2)

Table 2

Bayesian multinomial logistic regression model for mono- and co-infection with *Schistosoma mansoni* and hookworm with geostatistical random effects, based on parasitological data among 27,729 schoolchildren from 395 schools in East Africa.

Variable	β posterior mean (95% posterior CI)	OR posterior mean (95% posterior CI)
S. mansoni mono-infection		
Intercept	-3.838 (-4.696 - -2.888)	
Elevation	-1.050 (-1.507 - -0.550)	0.350 (0.222 - 0.577)
Distance to permanent water body	-1.475 (-2.353 - -0.793)	0.229 (0.095 - 0.452)
Urban-rural 3	-0.843 (-1.570 - -0.234)	0.430 (0.208 - 0.792)
Urban-rural 4	-0.477 (-1.492 - 0.367)	0.621 (0.225 - 1.444)
LST	-0.129 (-0.475 - 0.221)	0.879 (0.622 - 1.247)
Sex (female)	-0.154 (-0.269 - -0.038)	0.857 (0.764 - 0.963)
Age (9-10 years)	0.515 (0.315 - 0.721)	1.674 (1.370 - 2.057)
Age (11-13 years)	0.893 (0.725 - 1.060)	2.443 (2.064 - 2.886)
Age (≥14 years)	1.055 (0.785 - 1.312)	2.872 (2.192 - 3.714)
Phi (rate of decay)	3.517 (1.727 - 7.214)	
Variance of spatial random effect	6.388 (3.523 - 11.780)	
Hookworm mono-infection		
Intercept	-0.636 (-1.135 - -0.323)	
Elevation	-0.260 (-0.429 - -0.113)	0.771 (0.651 - 0.893)
Distance to permanent water body	-0.063 (-0.277 - 0.142)	0.939 (0.758 - 1.153)
Urban-rural 3	-0.016 (-0.386 - 0.317)	0.984 (0.680 - 1.373)
Urban-rural 4	0.150 (-0.194 - 0.593)	1.162 (0.824 - 1.810)
LST	-0.513 (-0.686 - -0.330)	0.599 (0.504 - 0.719)
Sex (female)	-0.094 (-0.151 - -0.034)	0.910 (0.860 - 0.966)
Age (9-10 years)	0.153 (0.043 - 0.261)	1.165 (1.044 - 1.298)
Age (11-13 years)	0.435 (0.329 - 0.539)	1.545 (1.390 - 1.714)
Age (≥14 years)	0.631 (0.489 - 0.762)	1.880 (1.630 - 2.143)
Phi (rate of decay)	4.980 (3.383 - 7.332)	
Variance of spatial random effect	1.311 (0.984 - 1.760)	
S. mansoni and hookworm co-infection		
Intercept	-4.352 (-5.024 - -3.744)	
Elevation	-1.206 (-1.626 - -0.754)	0.299 (0.197 - 0.471)
Distance to permanent water body	-1.203 (-1.736 - -0.546)	0.300 (0.176 - 0.579)
Urban-rural 3	-0.499 (-1.037 - 0.024)	0.607 (0.355 - 1.024)
Urban-rural 4	-0.290 (-1.165 - 0.481)	0.748 (0.312 - 1.618)
LST	-0.563 (-1.170 - -0.139)	0.570 (0.310 - 0.870)
Sex (female)	-0.364 (-0.465 - -0.259)	0.695 (0.628 - 0.772)
Age (9-10 years)	0.597 (0.416 - 0.791)	1.816 (1.516 - 2.206)
Age (11-13 years)	1.096 (0.937 - 1.259)	2.992 (2.553 - 3.522)
Age (≥14 years)	1.344 (1.103 - 1.581)	3.834 (3.013 - 4.860)
Phi (rate of decay)	3.758 (2.101 - 7.363)	

Variable	β posterior mean (95% posterior CI)	OR posterior mean (95% posterior CI)
Variance of spatial random effect	6.339 (3.977 - 9.954)	

Europe PMC Funders Author Manuscripts